Foliation development and hydrothermal gold emplacement in metagabbroic rocks, central Yukon, Canada

Doug MacKenzie[1], Dave Craw
Geology Department, University of Otago, Dunedin, New Zealand

Colin Brodie
Mendoza, Argentina

Adrian Fleming
Rockworks Ltd., Vancouver, Canada

MacKenzie, D., Craw, D., Brodie, C., and Fleming, A., 2013. Foliation development and hydrothermal gold emplacement in metagabbroic rocks, central Yukon, Canada. *In:* Yukon Exploration and Geology 2012, K.E. MacFarlane, M.G. Nordling, and P.J. Sack (eds.), Yukon Geological Survey, p. 47-64.

ABSTRACT

Gold mineralization has been identified on the foliated margins of Paleozoic gabbroic intrusions, where a protracted series of structural preparation events has enhanced rock permeability. Rheological contrasts between these mafic rocks and amphibolite facies metasedimentary hosts have resulted in variable foliation development, especially at margins of mafic bodies. Initial foliation development centred on granitoid material in magmatic intrusion breccia, and was enhanced by syn-metamorphic biotite formation. Early mineralized quartz vein development occurred under greenschist facies conditions during and/or after regional Mesozoic thrust stacking of kilometre scale rock slabs. Initial vein emplacement was largely controlled by the foliation in mafic gneiss, and minor chloritic alteration and later hydrothermal generations cut across all structures. Gold mineralization involved only minor introduction of As, Sb, and S, and the hosting quartzite has higher As, Sb, and S content than most mineralized veins. Au is accompanied by elevated Bi, Mo, and Te in quartz veins.

[1]*doug.mackenzie@otago.ac.nz*

INTRODUCTION

Recent research and gold exploration near to new Yukon gold discoveries in the White River area (MacKenzie *et al.,* 2010; Wainwright *et al.,* 2011; Fig. 1) has highlighted the presence of abundant mafic and ultramafic rocks (MacKenzie and Craw 2012); some of these mafic rocks have elevated gold concentrations worthy of serious exploration attention. This style of mafic-hosted gold mineralization required a protracted chain of structural preparation events to enhance rock permeability. The nature of this structural preparation is well displayed in these rocks, and the processes that have occurred are relevant to all metamorphosed mafic bodies around the world. This paper provides an outline of the processes of structural preparation that have led to localized gold enrichment. In particular, foliation development, and its subsequent control on vein emplacement, has been important in gold localization in these mafic bodies. Geochemical observations on the nature of this new

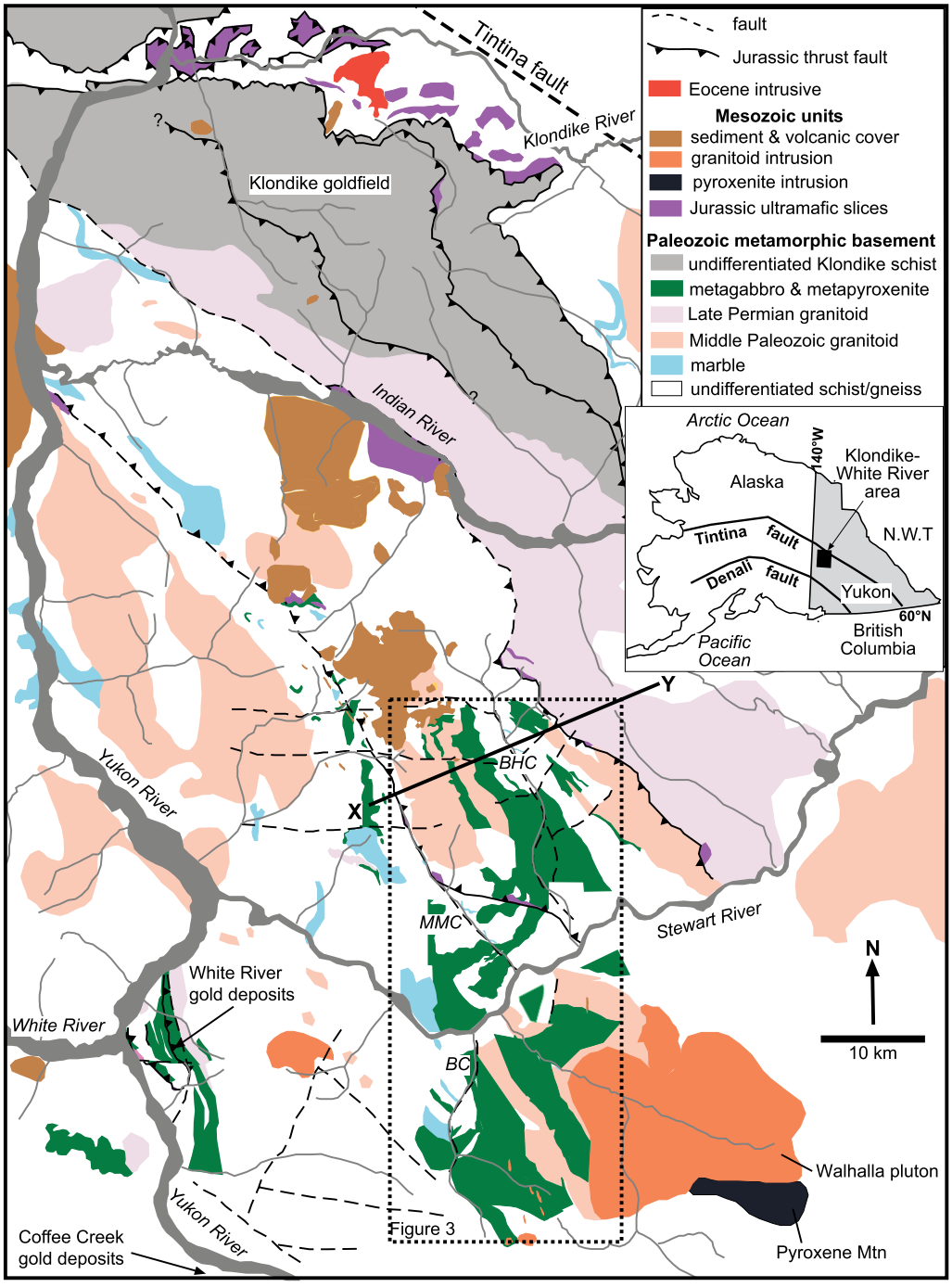

Figure 1. *Summary geological map of the Yukon-Tanana terrane in west-central Yukon, showing the geological relationship between the Klondike gold field and significant new gold deposit discoveries farther south (White River and Coffee Creek deposits). The area of this study is depicted in cross section (line X-Y; Fig. 2a) and in the dotted box (Fig. 3), where significant placer gold bearing creeks (Black Hills Creek (BHC); Maisy May Creek (MMC); Barker Creek (BC)) imply undiscovered deposits. Inset shows the location of this area in NW North America.*

type of hydrothermal gold deposit are provided to help to characterize the hydrothermal system in this largely unexplored part of the Yukon-Tanana terrane.

GENERAL GEOLOGY

The basement rocks in central Yukon are part of the Yukon-Tanana terrane, which is a metamorphic complex including mafic and felsic plutons (Figs. 1 and 2a; Mortensen, 1992, 1996; MacKenzie *et al.,* 2008a, 2010; Table 1). The metamorphic complex consists of metasedimentary rocks, including quartzite, marble, and metaclastic micaceous schist, that were intruded by granitoids and gabbroic rocks prior to and/or during Paleozoic metamorphism (Mortensen, 1992, 1996; Ryan and Gordey, 2004; Ruks *et al.,* 2006). At least three stages of granitoid intrusion occurred between the Devonian and Permian (Ruks *et al.,* 2006), and mafic intrusions apparently accompanied all of these intrusive events. Variable development of foliation during metamorphism yielded a prominent polyphase foliation in most rocks, although some of the more massive rocks have remained unfoliated. Metamorphic grade ranges from greenschist facies in the north, around the main Klondike goldfield (Fig. 1; Mortensen, 1992, 1996; MacKenzie *et al.,* 2008a) to amphibolite facies farther south in the White River and Stewart River areas (Ryan and Gordey, 2004; Ruks *et al.,* 2006; MacKenzie *et al.,* 2010). The present study was conducted entirely in amphibolite facies rocks previously mapped on a regional scale by Ryan and Gordey (2004).

The metamorphic basement was disrupted and stacked on a kilometre scale by thrusting in the Jurassic, and slices of mafic and ultramafic rocks of the Slide Mountain terrane, and some Triassic sedimentary units in the north were incorporated (Figs. 1 and 2a; Table 1; Mortensen, 1990, 1996). This thrust stacking occurred under greenschist facies conditions, along with the associated development of greenschist facies shear and fold zones (MacKenzie *et al.,* 2008a). Minor intrusion of granitoid and associated mafic bodies accompanied this Jurassic collisional orogenesis. However, pyroxenite sills and related amphibolite bodies in the White River area (MacKenzie *et al.,* 2010), previously presumed to be Jurassic in age, are almost certainly part of the suite of Paleozoic mafic bodies described in this study (MacKenzie and Craw, 2012).

Compressional tectonics gave way to regional extension in the Cretaceous, and persisted through to the Eocene (Table 1). Minor mafic and/or felsic volcanism and associated shallow intrusion accompanied this extension (Gabrielse and Yorath, 1991; Mortensen, 1996; Table 1). The Tintina fault, a major regional transcurrent structure (Fig. 1), accommodated mainly Eocene age displacement, which has offset parts of the Yukon-Tanana terrane by ~400 km (Gabrielse *et al.,* 2006). Regional uplift and erosion following movement along the Tintina fault

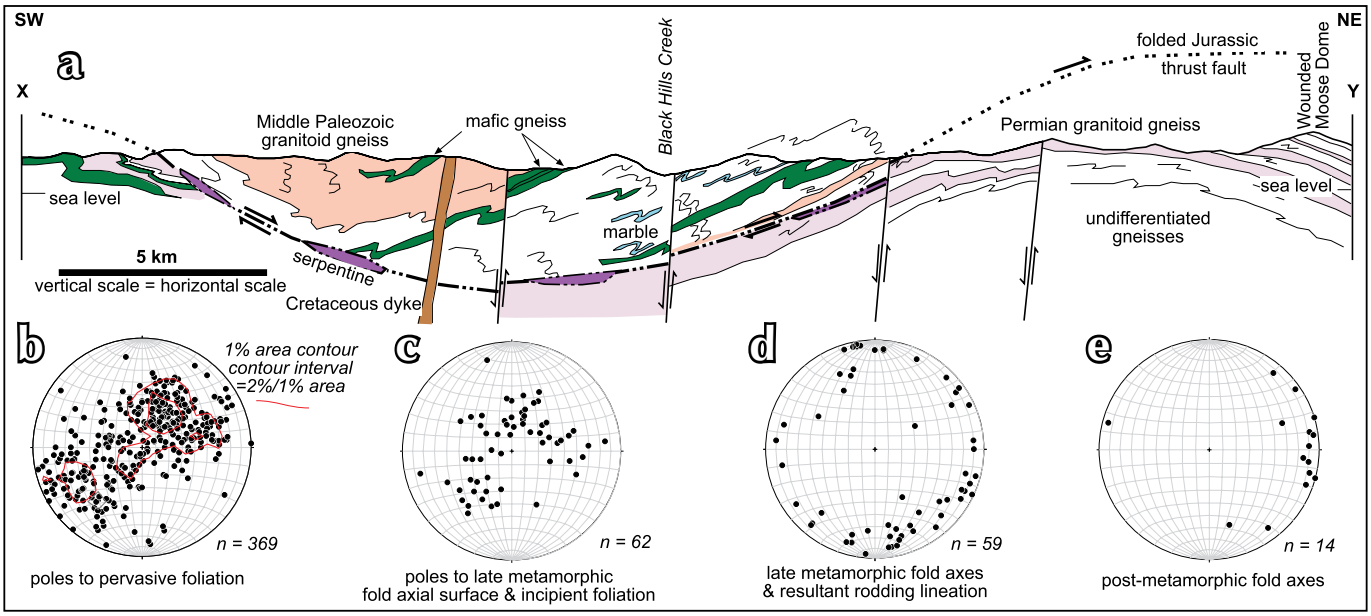

Figure 2. *Cross section and stereonets. a) X-Y line in Fig. 1, rock units depicted in the same colours as Fig. 1. Stereonets: b) lower hemisphere stereographic projection of poles to the pervasive metamorphic foliation; c) poles to late metamorphic planar fabric; d) late metamorphic linear features; and e) post-metamorphic fold axes.*

Table 1. *Summary of the principal geological events affecting mafic rocks and hosting metasediments in the central Yukon-Tanana terrane (Figs. 1 and 3).*

Age	Unit/event	Tectonics (Regional* structural event)	Associated intrusions	Metamorphism	Gold	Structure	Granitoid orthogneiss	Metasediment key minerals	Mafic gneiss key minerals
Pliocene-Recent	White Channel and modern gravels	Regional uplift and erosion		Groundwater alteration	Placer	Fault reactivation with gouge	Fault gouge, cataclasite, chloritic alteration with pyrite, carbonates & clays	Fault gouge, cataclasite, chloritic alteration with carbonates & clays	Fault gouge, cataclasite, chloritic alteration with clays (see Table 3)
Eocene		Regional extension (D_3)	Dykes	Hydrothermal alteration	?	Normal faults with cataclasite & gouge			
Late Cretaceous	Carmacks andesitic volcanism			Hydrothermal alteration	Epithermal				
Middle Cretaceous	Indian River fluvial		Ignimbrites and feeders	Groundwater alteration	Paleoplacer				
Jurassic-Cretaceous?	White River mineralization	?	?	Hydrothermal alteration	Disseminated; veins	Fault-hosted breccias	Hematitic, sericitic alteration ± pyrite	Graphite, pyrrhotite, pyrite (quartzite)	Fuchsite, chlorite, pyrite
Jurassic	Slide Mountain terrane collision and thrusting	(D_4) Orogenic collision, uplift, thrust stacking (D_3)		Hydrothermal alteration	Orogenic veins	Late folds, fractures, breccias	Shearing, with epidote, chlorite, hematite, pyrite, magnetite		Ankerite, pyrite (in Klondike)
			Granite plutons; pyroxenite	Greenschist facies (propylitic)	Localized mobility?	Brittle-ductile shearing		Epidote, quartz, albite, hematite, magnetite (schist); Graphite, pyrrhotite, pyrite (quartzite); diopside, actinolite, epidote (marble)	Epidote, quartz, actinolite, albite, hematite, magnetite; local skarn against marble
				Localized greenschist facies		Ultramafic slice emplacement with shearing			
Permian	Late metamorphic mafic intrusion	Assembly of Yukon-Tanana terrane (D_1-D_2)	Felsic segregations; augen granite	Amphibolite facies		Folding, rodding of foliation	Variable foliation, folding	Garnet, Al-silicates (micaceous schist); hornblende, garnet, graphite (quartzite)	Pyroxene to hornblende (unfoliated); hornblende, biotite, garnet;
Late Paleozoic	Pre-syn metamorphic mafic intrusion		Felsic segregations; augen granite			Main foliation (polyphase)	Variable foliation		
Early Paleozoic?	Host rock sedimentation	?			Syn-depositional enrichment?	Bedding			

*after MacKenzie *et al.*, 2010; MacKenzie and Craw, 2012

has resulted in formation of the productive gold placer deposits of the Klondike area, and tributary valleys of the Stewart River to the south, particularly Black Hills, Maisy May, and Barker creeks (Fig. 3; Fuller and Anderson, 1992; Chapman *et al.,* 2011). The source(s) of the gold for the abundant placer deposits is presumed to be the Jurassic orogenic veins in the Klondike area (Lowey, 2005; MacKenzie *et al.,* 2008a; Chapman *et al.,* 2011) and other scattered hydrothermal deposits of unknown affinity, such as the recently-discovered White River and Coffee Creek deposits (MacKenzie *et al.,* 2010; Wainwright *et al.,* 2011; Fig. 1). The current small size of these newly discovered bedrock deposits points to the probable existence of other undiscovered deposits (Chapman *et al.,* 2011), and this observation has been driving a modern "gold rush" in the area.

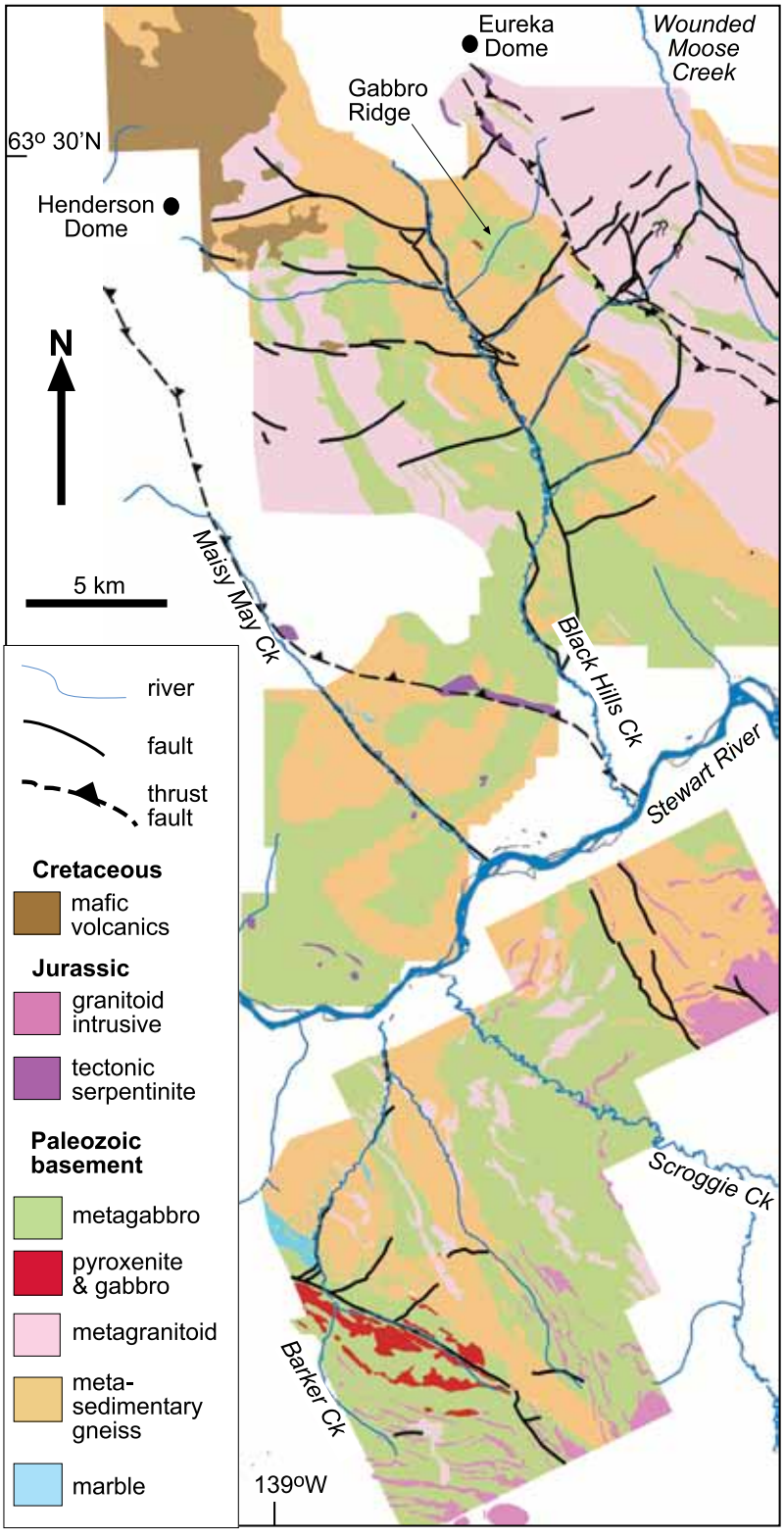

Figure 3. *Geological map of the study area showing the surface distribution of metagabbro (green) and relict pyroxenite (red) in relation to other rock types in the area.*

METHODS

Results of extensive new field mapping, sampling, and geochemical analysis over an area >500 km^2 centred on the auriferous Black Hills Creek and Barker Creek catchments of the Stewart River area, a previously little-studied area near to the White River gold discovery (Figs. 1, 2, and 3) are incorporated in this paper. This research is an extension of a regional scale project on structural and lithological mapping and gold deposit investigations (MacKenzie *et al.,* 2008a, 2010; MacKenzie and Craw, 2012). Field mapping was supplemented by exploration soil geochemistry on ridges and spurs using lithological discriminants. Lateral continuity of rock units was determined from airborne geophysical surveys, of which the magnetic and potassium radiometric data were most useful for map construction (Fig. 3). Rock exposure was created in exploration trenches, and two cored drillholes were emplaced in mafic rocks on Gabbro Ridge (Fig. 3; informal name) where soil, surface rock, and trench mapping and sampling had defined a significant gold anomaly (up to 10 ppm Au). Pulps from samples of altered rock were fused with lithium metaborate, dissolved in nitric acid, and analysed using ICP-MS. Gold was determined to be present in surface rocks and trench wall samples (~50-250 g) by fire assay, using an atomic absorption finish. All analyses were done at Acme Analytical Labs in Vancouver, Canada.

STRUCTURE

The gneiss in the mapped area has a near-pervasive amphibolite facies metamorphic foliation that has shallow to moderate dips to northeast and southwest (Fig. 2a,b). This foliation defines the fold axial surface to synmetamorphic recumbent ductile folds. Late metamorphic recumbent folding has caused localized disruption of the main foliation, and some development of a new foliation in tight fold hinges. This incipient late foliation also has shallow dips (Fig. 2c), but is oblique to the main foliation. The late metamorphic folding and foliation development has caused a prominent rodding lineation fabric to dominate

some outcrops, due to intersection of the two foliations. Late metamorphic fold axes and the associated rodding lineations have a wide range of orientations (Fig. 2d), which have been controlled by local rheological differences in the rock mass rather than regional tectonic stress orientations.

The metamorphic structure has been disrupted by greenschist facies shearing, most of which is concentrated into narrow zones associated with Jurassic thrust faults (Figs. 1, 2a, and 3). These sheared and retrogressed zones include sporadic slices of variably serpentinized ultramafic rock that is internally sheared into phacoidal blocks on the 1-10 m scale. Subordinate greenschist facies shear zones, brecciated fault zones, and veins hosted in these structures, cut steeply across the amphibolite facies gneiss between the shallow-dipping thrust faults. The gneissic foliation and the Jurassic thrust faults have been folded into broad (10 km scale) open upright antiforms and synforms by post-metamorphic compressional deformation (Fig. 2a). This folding is partly responsible for the great-circle scattering of foliation orientations, with a general northwest fold axis trend (Figs. 1 and 2a), although most of this scatter is a result of late-metamorphic folding (Fig. 2a,c). Minor folding of foliation, associated with this deformation, occurs at outcrop scale but these structures are relatively rare and have widely-varying trends (Fig. 2e). The regional upright folds are disrupted by numerous normal faults spaced on the 1-10 km scale, with irregular and intersecting orientations (Figs. 1, 2a, and 3).

HOST ROCKS FOR MAFIC INTRUSIONS

The metasedimentary gneiss host rocks are dominated by quartzite, which ranges from almost pure quartz to muscovite-rich (~10%) variants. The quartzite is apparently derived from quartz-rich clastic sediments, as relict pebbles and sand grains are rarely preserved in low-strain domains (Fig. 4a). However, most quartzite is pervasively recrystallized and is variably foliated, depending on the muscovite content. Minor metamorphic graphite accompanies muscovite in the foliation, along with scattered pyrrhotite, pyrite, sphalerite, galena, arsenopyrite, and chalcopyrite. Interlayered micaceous schist includes muscovite-rich and biotite-rich variants, and both types locally contain subordinate garnet and kyanite or sillimanite. Micaceous schist is strongly foliated, and late metamorphic folding has induced a near-pervasive late metamorphic fold axial surface foliation that largely obscures the earlier metamorphic foliation(s) in some outcrops. The schist in these refoliated zones is commonly strongly lineated parallel to the intersection of the foliations (Fig. 2d).

Marble is less common than quartzite, but is locally interleaved with quartzite on the 1-50 m scale (Figs. 1, 2a, and 3). The marble is calcite-rich, with subordinate muscovite, biotite, and quartz. Some calcareous quartzite horizons (1-5 m) occur where quartzite and marble are interlayered. Foliation is typically weakly developed because of the relative paucity of micas, but layering defined by mineralogical variations has been folded and refolded during complex structural and metamorphic reconstitution.

Gneissic metagranitoid intrusions into the metasedimentary host rocks (Table 1; Figs. 1, 2a, and 3) locally form host rocks for the mafic gneiss, although the metamorphic overprint generally obscures the relative timing of emplacement of these intrusive rocks. The metagranitoid rocks are dominated by plagioclase, quartz, biotite, and hornblende, and potassium feldspar augen in some bodies. Foliation-parallel horizons of gneissic metagranitoid rocks are interleaved with mafic gneiss on the centimetre to metre scale, and vice versa.

MAFIC INTRUSIONS

Mafic gneiss bodies are widespread in the study area, and locally dominate outcrop over large areas (Fig. 3). This dominance in map pattern is partly a result of the shallow dipping foliation (Fig. 2a,b) and the relative resistance of mafic gneiss to erosion. This has left many ridges made up of mafic rocks, and they are underlain by less resistant rock types that have eroded to form valleys (Fig. 3). The contact between the mafic rocks and their hosting metasedimentary gneiss, one of the principal topics of this study, is therefore a shallow-dipping and sinuous feature around the modern topography (Fig. 3). Likewise, the relationship between mafic gneiss and metagranitoid bodies is generally relatively simple foliation-parallel interlamination (Fig. 2a), although the topographic effects lead to a complex map pattern (Fig. 3).

Synmetamorphic deformation is inhomogeneous in the basement rocks, and some portions of the mafic bodies are preserved with little or no overprinting foliation. The most intact bodies are those that were emplaced late in the metamorphic sequence, after the main foliation development. These late-stage bodies are variably foliated

internally and on their margins, but still retain undeformed pods on the 0.5 to 100 m scale in which the metamorphic overprint is minor. The undeformed pods occur within zones of mafic gneiss that can be several kilometres wide in map view (Fig. 3), with maximum thickness poorly defined.

Undeformed pods in mafic bodies commonly consist of unfoliated gabbro with coarse grained (cm scale) clinopyroxene, orthopyroxene, and/or hornblende, and variable amounts of plagioclase (Figs. 5 and 6). No olivine has been observed in these rocks. Pyrrhotite is a common accessory mineral (typically 1-5%) within even the least-deformed and metamorphosed metagabbro and pyroxenite, and may have been a primary magmatic mineral. Mafic intrusion breccia is abundant, in which previously-emplaced mafic rocks have been invaded and disrupted by later mafic intrusive rocks. Pyroxenite sills up to 5 m thick are preserved where they have been intruded parallel to late metamorphic fold axial surfaces, with only minor (<1 m) marginal recrystallization and foliation development.

Mafic intrusions are almost invariably accompanied by conspicuous granitoid intrusive rocks, forming xenolithic breccia with a granitoid matrix (Fig. 5c). The xenolithic breccia generally has a wide range of clast types, including mixtures of metagabbro, pyroxenite, earlier granitoid rocks (Fig. 5c), and some metasedimentary xenoliths. Some mafic clasts have a biotite-rich reaction zone (mm scale) on their rims (Fig 5c). The granitoid matrix is dominated by plagioclase and quartz, with subordinate biotite and hornblende. Similar granitoid rocks also cut across the mafic bodies as centimetre to metre scale dykes with irregular orientations, or are locally emplaced as sills parallel to pre-intrusion foliation.

All the mafic bodies have some degree of foliation development on their margins, and foliated zones occur throughout the bodies on the 1-10 m scale. Hornblende recrystallization and biotite growth are key drivers of foliation development (Fig. 6). Granitoid rocks within the mafic bodies become foliated before immediately adjacent metagabbro, because of the primary biotite and quartz content (Fig. 7a). Foliation development in mafic rocks is enhanced by recrystallization and alignment of biotite on the margins of mafic clasts in xenolithic breccia (Fig. 7b,c). Pyrrhotite in mafic rocks has been recrystallized into parallelism with the developing foliation, and locally forms veins that cut across the foliation, and is commonly accompanied by minor pyrite. Later pyrite veinlets cut across pyrrhotite-rich rocks.

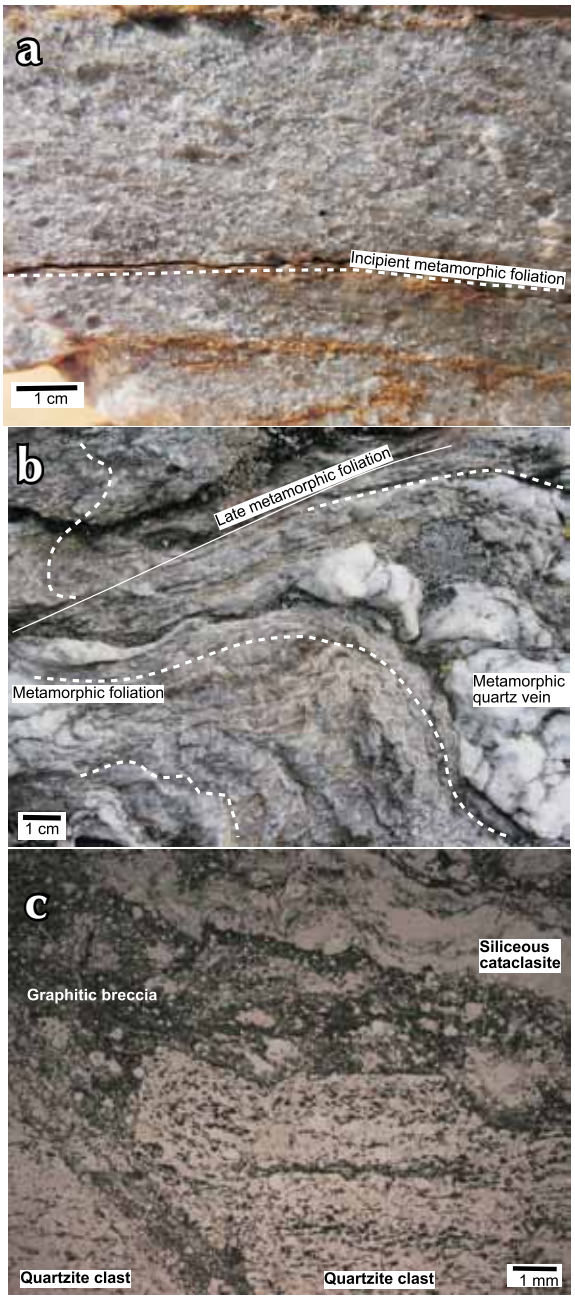

Figure 4. *Photographs of textures of quartzite host rocks to metagabbro. a) Little-deformed pod of quartzite showing remnants of clastic texture, with only incipient foliation development (white dashed line). b) Fully recrystallized quartzite with a late metamorphic fold of the metamorphic foliation (white dashed line) and a metamorphic foliation-parallel quartz vein. Incipient late metamorphic foliation (solid white line) has developed parallel to the fold axial surface. c) Photomicrograph (plane polarized light) of brecciated graphitic quartzite at the margin of a metagabbro body. Amphibolite facies graphitic foliation (black visible in the clast at bottom); the matrix consists of breccia cemented by hydrothermal graphite, and siliceous cataclasite.*

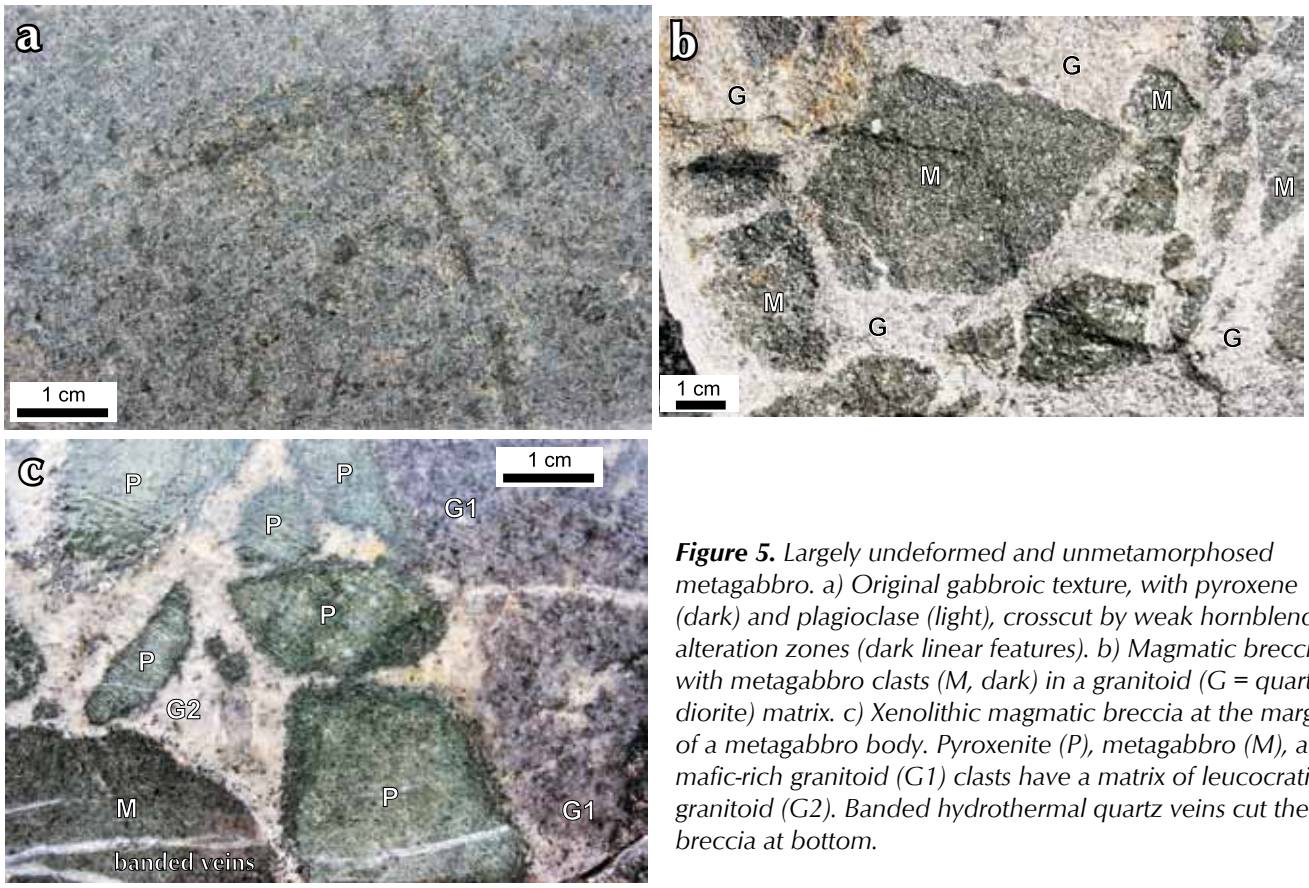

Figure 5. *Largely undeformed and unmetamorphosed metagabbro. a) Original gabbroic texture, with pyroxene (dark) and plagioclase (light), crosscut by weak hornblende alteration zones (dark linear features). b) Magmatic breccia, with metagabbro clasts (M, dark) in a granitoid (G = quartz diorite) matrix. c) Xenolithic magmatic breccia at the margin of a metagabbro body. Pyroxenite (P), metagabbro (M), and mafic-rich granitoid (G1) clasts have a matrix of leucocratic granitoid (G2). Banded hydrothermal quartz veins cut the breccia at bottom.*

The amphibolite facies foliation has undergone minor reactivation under greenschist facies conditions, with associated chloritization of biotite and relict hornblende, resulting in narrow (cm to m scale) chloritic shear zones. These are typically discontinuous at the outcrop scale, although they are more common and continuous near to the regional serpentinite-bearing thrust faults that stacked basement rocks in the Jurassic (Fig. 1 and 2a).

BRITTLE DEFORMATION AND HYDROTHERMAL ALTERATION

SHEARS, VEINS, AND BRECCIA

The late metamorphic structural zones within, and along the margins of, metagabbro bodies are the locus for subsequent more brittle deformation and hydrothermal alteration. This alteration was initiated under greenschist facies metamorphic conditions, with recrystallization of hornblende and biotite to epidote and chlorite, locally with hematite, magnetite and/or pyrite (Tables 1 and 2). The early stages of this alteration occurred along the foliation, with syn-alteration deformation that caused a weak shear foliation to develop locally. This type of alteration spread into veins and adjacent wall rocks of brittle structures such as fractures, breccia, and faults that developed in the metagabbro (Table 1) and adjacent foliated and folded quartzite. Some such quartz veins contain minor pyrite, chalcopyrite, and rare galena.

Several generations of veins and breccia developed after this early evolution to a brittle deformation regime (Tables 1 and 2). The earliest of these generations in the metagabbro bodies does not affect the mafic rocks, but does affect some of the granitoid dykes and granitoid-rich breccia. This hydrothermal generation resulted in emplacement of a set of thin (millimetre scale) massive quartz veins, exhibiting alteration haloes that typically extend for ~1 cm from the veins (Fig. 8a). Alteration is dominated by chloritization of biotite, and associated sericite and minor pyrite. Zones of more extensive rock alteration occur where several haloed veins intersect, and the alteration zones merge into bleached and partially silicified rock with sericite and remnants of chlorite (Fig. 8a). Similar chloritic and sericitic haloes and bleaching occur within some nearby granitoid gneiss, locally with pyritic alteration. This chloritic alteration resembles, but

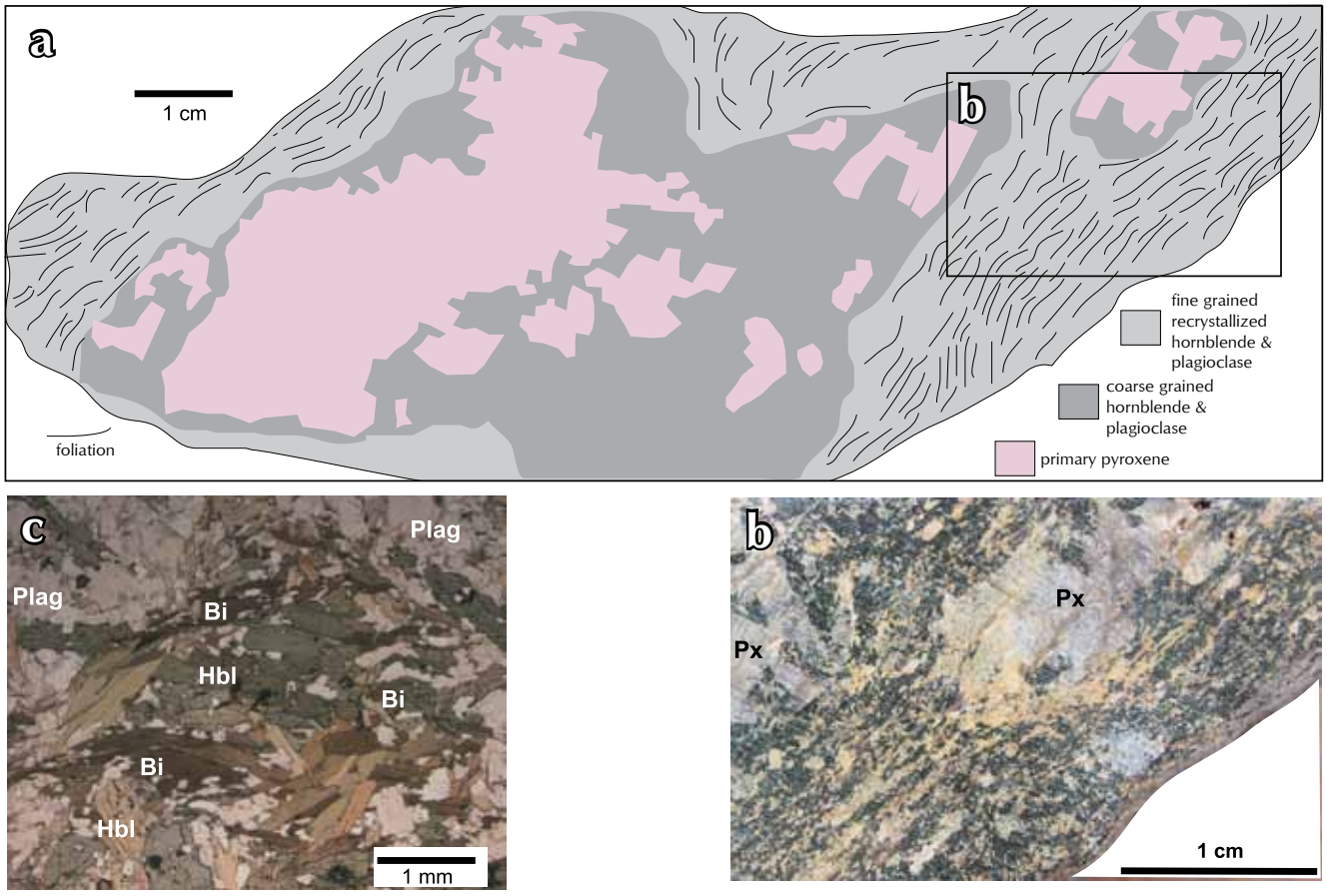

Figure 6. *Textures of metamorphism and foliation development in metagabbro. a) Block from outcrop showing a relict coarse grained pyroxenite core surrounded by unfoliated coarse hornblende metagabbro. Finer grained foliated hornblende metagabbro surrounds the unfoliated rocks. b) Close-up view of a part of the block in (a), showing the steep gradient from primary rock to foliated hornblende metagabbro. c) Photomicrograph (crossed polars) of foliated hornblende metagabbro, showing the localized formation of metamorphic biotite that dominated foliation development.*

structurally post-dates, texturally similar hematitic sericitic alteration of granitoid gneiss that occurs in the same area and, contains gold in the White River area (Table 1).

A later generation of massive quartz veins (Table 2) is more extensive, but lacks distinct alteration haloes (Fig. 8b,c). These massive veins are generally small (millimetre-centimetre scale), and discontinuous, with some included host rock fragments as breccia clasts (Fig. 8b,c). Most of these veins have nucleated in foliated granitoid, or on boundaries between foliated granitoid and variably foliated mafic clasts in xenolithic breccia, where they are largely controlled by foliation (Fig. 8b,c). Margins of these veins, and most breccia fragments, have incipient chloritic alteration of biotite and/or hornblende. Gold-bearing quartz vein material collected from surface zones on mafic rocks contain pyrite and have irregular margins that partially incorporate foliated but weakly chloritized hornblende metagabbro, and formed sub-parallel to foliation. These gold-bearing samples are similar to the massive quartz veins, especially resembling that in Figure 8c.

All rock types in the mafic bodies are crosscut by a prominent but volumetrically small set of quartz veins that are generally banded due to polyphase opening and mineralization history. The banded veins commonly contain prismatic quartz crystals in open cavities, and variable amounts of euhedral pyrite. Most banded veins formed with steep dips, at a high angle to the foliation (Fig. 8b-d). However, these veins also exploit other rock weaknesses, such as foliation and margins of pre-existing veins (Fig. 8c). Some banded veins have formed preferentially in massive rocks such as unfoliated metagabbro and pyroxenite (Fig. 5c).

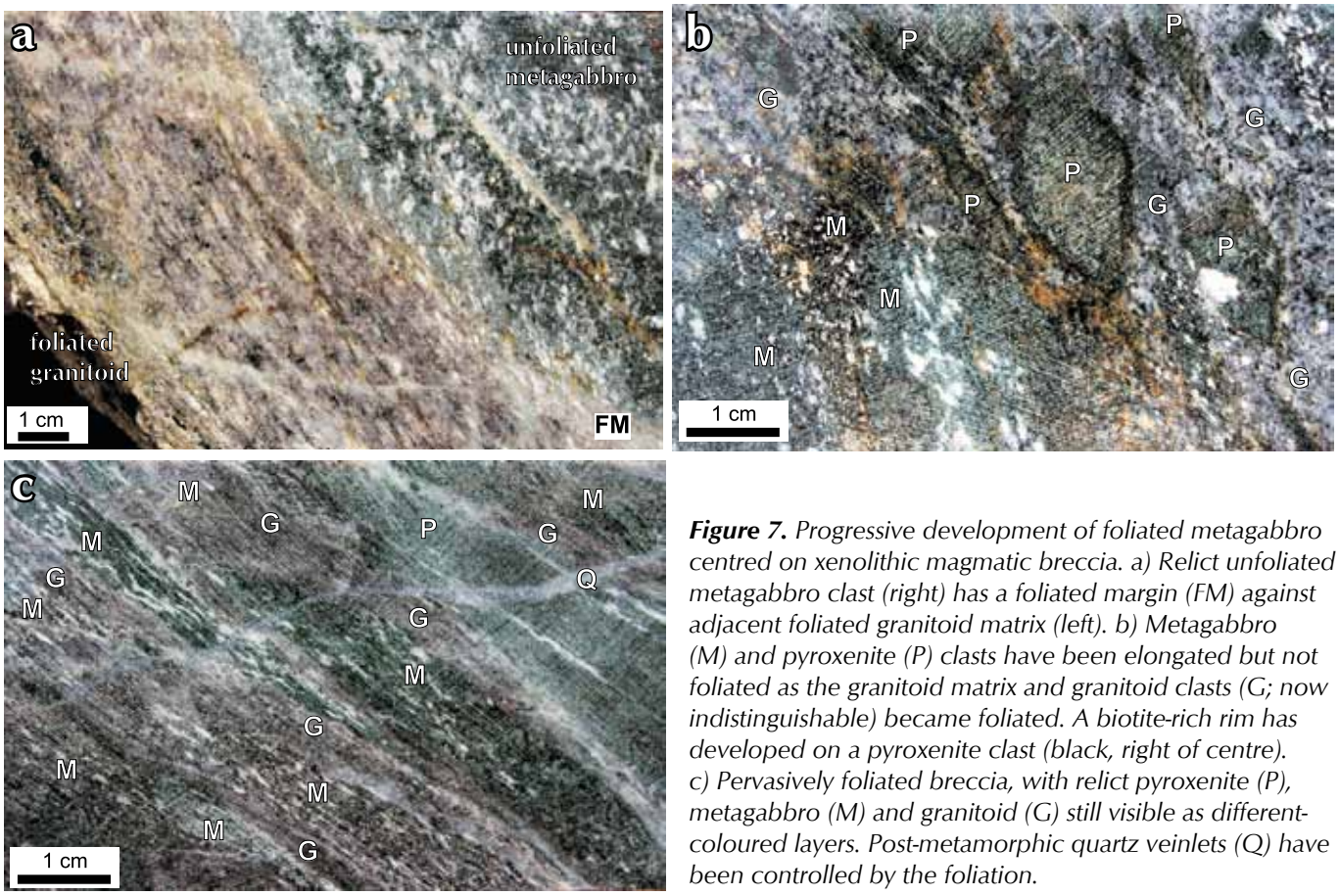

Figure 7. *Progressive development of foliated metagabbro centred on xenolithic magmatic breccia. a) Relict unfoliated metagabbro clast (right) has a foliated margin (FM) against adjacent foliated granitoid matrix (left). b) Metagabbro (M) and pyroxenite (P) clasts have been elongated but not foliated as the granitoid matrix and granitoid clasts (G; now indistinguishable) became foliated. A biotite-rich rim has developed on a pyroxenite clast (black, right of centre). c) Pervasively foliated breccia, with relict pyroxenite (P), metagabbro (M) and granitoid (G) still visible as different-coloured layers. Post-metamorphic quartz veinlets (Q) have been controlled by the foliation.*

Rare veinlets (sub-millimetre scale) containing iron-bearing carbonate cut across the banded veins at a variety of angles in mafic rocks, especially in granitoid-bearing xenolithic breccia. These veinlets also contain minor pyrite and quartz. Late stage pyrite-bearing clay-rich coatings, with disseminated calcite, have formed on fracture surfaces that cut across all of the above vein generations (Table 2).

Brecciated graphitic quartzite, immediately adjacent to metagabbro bodies, is variably silicified and cemented by hydrothermal quartz (Fig. 4c), forming brittle rocks that are locally re-brecciated and re-silicified. Hydrothermal graphite accompanied the silica cementation, and this graphite locally dominates the breccia matrix (Fig. 4c). Scattered micron-scale grains of pyrrhotite and pyrite occur in the graphitic breccia cement.

The mafic/metasediment boundaries, and other foliated zones, were locally reactivated by an unknown number of brittle fault generations that may be as young as Quaternary. These fault zones consist of a complex set of gouge and breccia (metre scale) made up of polyphase soft, clay-rich uncemented cataclasite derived from the immediate wall rocks. Adjacent rocks are generally highly fractured, and hydrothermal fluids have deposited minor quartz (locally prismatic) and scattered euhedral pyrite grains on fracture surfaces. Chlorite-calcite, or hematite-chlorite-calcite coatings occur on shear-polished surfaces in fault zones cutting mafic bodies. Several of these faults cut across the regional metamorphic fabric (Figs. 1, 2, and 3), and associated minor faults have reactivated the foliation in adjacent gneiss, forming foliation-parallel gouge zones.

SKARNS

Localized reaction skarn zones have developed at some boundaries between metagabbro and marble, on the 1-20 m scale. These reaction skarns are larger scale than those that occur in marble xenoliths in metagabbro. In contrast, there is little or no skarn development between marble and interlayered quartzite, or marble and interlayered mafic gneiss, in many other parts of the metamorphic sequence. Most of these marble boundaries

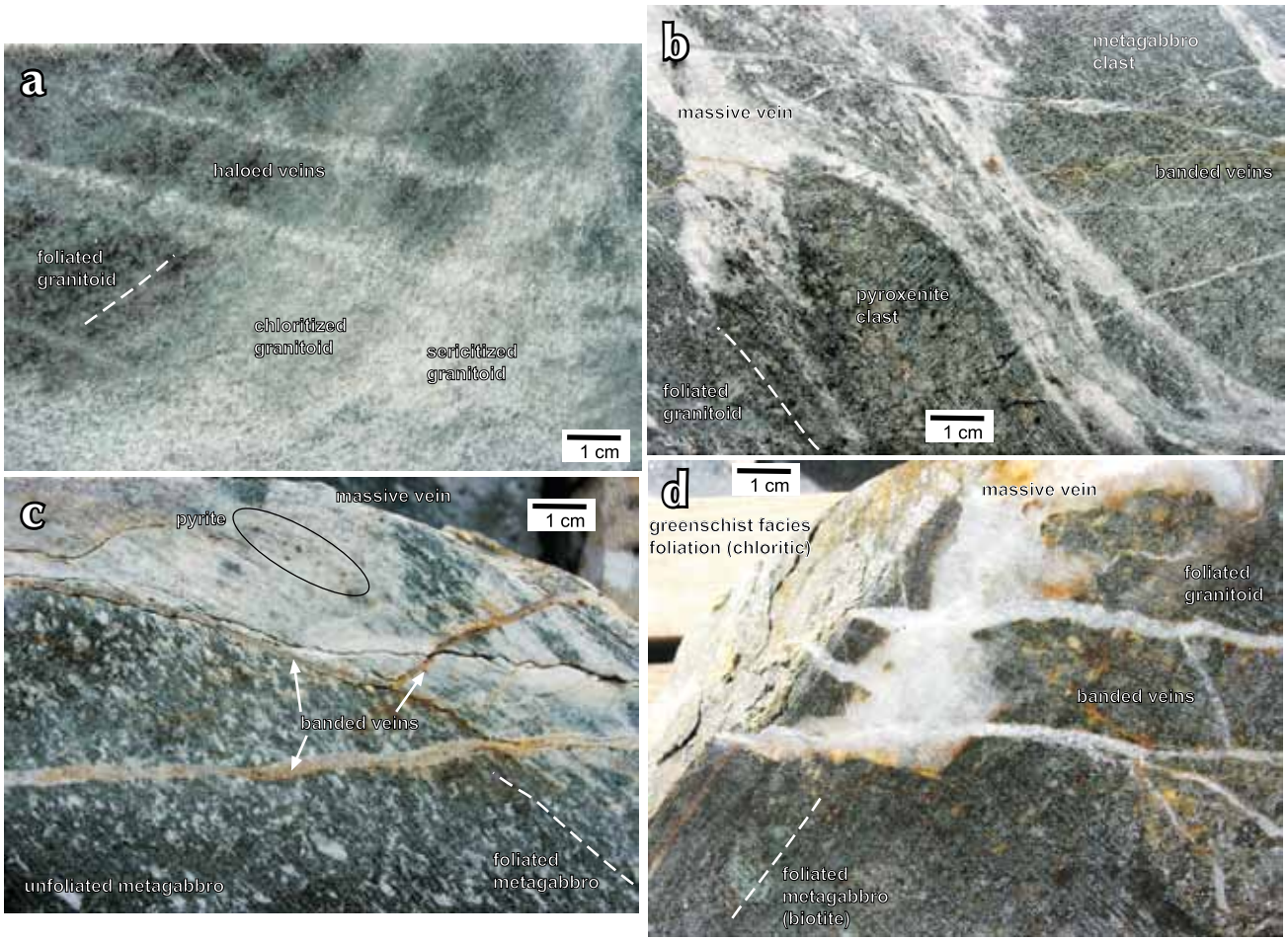

Figure 8. *Hydrothermal vein generations in weakly mineralized metagabbro near a body margin on Gabbro Ridge (Fig. 3). a) Pale chlorite-sericite-quartz seams with alteration haloes cut weakly foliated granitoid in a magmatic breccia. b) Massive quartz veins with minor pyrite have nucleated in foliated granitoid between mafic clasts. Later banded quartz veins cut across all rock types. c) Massive quartz vein with scattered pyrite has developed in the foliated part of metagabbro, with foliated metagabbro breccia clasts (right). A banded quartz vein has formed at the edge of the massive vein, and other banded veins cut all rock types. d) Massive quartz vein with minor pyrite has nucleated near the boundaries between biotite-foliated metagabbro and a chloritic shear zone on left and foliated granitoid on right. Later banded quartz veins cut across all rock types.*

are sharp and unreacted at even the millimetre scale. The reaction skarn zones are unfoliated, and skarn minerals cut across the metamorphic foliation and late metamorphic fold-related structures. Minor skarn recrystallization follows the metamorphic foliation on skarn margins, but skarn minerals have grown across that foliation. These observations suggest that skarn formation occurred during post-metamorphic hydrothermal alteration described in the previous section. The skarns are dominated by actinolite and epidote, with minor diopside, vesuvianite, and garnet. Pyrite and/or pyrrhotite are locally abundant as anhedral masses and veins. The best-developed skarns form massive hard rock zones that transgress the metamorphic foliation, with gradational (<1 m) boundaries to unreacted marble.

CHEMICAL ALTERATION

More than 1000 geochemical analyses of variably altered rocks at and near metagabbro boundaries were examined in this study. Most elements analysed have little variation in the altered rocks and are not useful for distinguishing gold mineralization near these boundaries. Variation of metal content among the variably altered rock types, at and near metagabbro margins and the associated quartz veins, are depicted in Figures 9 and 10. Lower results are omitted from the graphs in Figures 9 and 10 for clarity, especially when the low values are close to the practical detection limit for the analytical methods.

Table 2. *Principal vein generations that cut metagabbro and associated rocks, arranged in chronological order from bottom (oldest) to top (youngest).*

Vein generation	Principal minerals	Metallic minerals	Structure	Shape
late fractures	quartz, clay, calcite	pyrite	fracture-controlled	irregular
Fe carbonate	ankerite, quartz	pyrite	fracture-controlled	lenticular, some breccia
banded	quartz (prismatic, drusy), calcite	pyrite, Au?	mostly steep across foliation; some along foliation, some breccia	parallel-sided, dilational jogs, vein arrays & networks
massive	quartz, calcite, chlorite	pyrite, Au	nucleated in foliation, some breccia	irregular, some diffuse margins
haloed	quartz, chlorite, sericite, calcite	pyrite	steeply cut foliation	diffuse, joint-controlled
epidote	quartz, epidote, chlorite, calcite	hematite, magnetite, pyrite	parallel, perpendicular to foliation	diffuse, joint-controlled

There is a crude positive correlation between As and Sb in the altered rocks and associated quartz veins (Fig. 9a). In particular, the altered quartzite typically has the highest As and Sb content. Elevated As and Sb in altered micaceous schist is generally from samples taken close to, or interlayered with, quartzite; quartz veins with elevated As and Sb are mainly from quartzite host rocks near metagabbro boundaries. Localized hydrothermal mobility of As and Sb from quartzite, having elevated As and Sb backgrounds (MacKenzie *et al.,* 2010), into veins and nearby alteration zones is probably responsible for the widespread nature of the As and Sb anomalies (Fig. 9a). This effect is less pronounced for altered metagabbro samples, some of which have minor As enrichment but little Sb enrichment (Fig. 9a). Altered quartzite is weakly enriched in both Mo and Bi, as well as As (Fig. 9b,c). Some of this enrichment reflects elevated background levels of these metals (MacKenzie *et al.,* 2010). However, some of the quartz veins are enriched in Mo and/or Bi independent of the As content (Fig. 9b,c).

Despite this metallic enrichment, the altered rocks are not strongly enriched in sulphide minerals, and typical S content is near background of 0.1 wt % (Fig. 9d). Some pyritic quartz veins have up to 1.0 wt % S, as does weakly altered and pyritic micaceous schist (Fig. 9d). Elevated S and Fe in weakly altered metagabbro (Fig. 9d) at least partially reflects locally-abundant metamorphic pyrrhotite, although some hydrothermal pyrite occurs in metagabbro as well. Likewise, weakly elevated Cu and Ni in some altered metagabbro (Fig. 9e) at least partially reflect the metamorphic sulphide content: Cu in chalcopyrite, and Ni in solid solution in pyrrhotite in these Ni-rich rocks. There has been little or no enrichment of Cu and Ni in most quartz veins, or in the other altered rocks, apart from some chalcopyrite-bearing veins and altered quartzite (Fig. 9e). Similarly, neither Pb nor Zn are enriched in most veins or altered rocks. However, some quartzite has metamorphic sphalerite and/or galena (MacKenzie *et al.,* 2010), and remobilization of these minerals may have resulted in localized enrichment of Pb and Zn (Fig. 9f). Galena occurs locally in veins in altered metagranitoid, resulting in minor Pb enrichment.

The strongest Au enrichment occurs in quartz veinlets, and there is only minor dissemination of gold in altered host rocks (Fig. 10a). This gold enrichment was not accompanied by significant As enrichment (Fig. 10a). However, gold-bearing veinlets, and some altered quartzite, are distinctly enriched in Mo and Bi (Fig. 10b,c). Likewise, the gold-bearing veins are also enriched in Te (Fig. 10d).

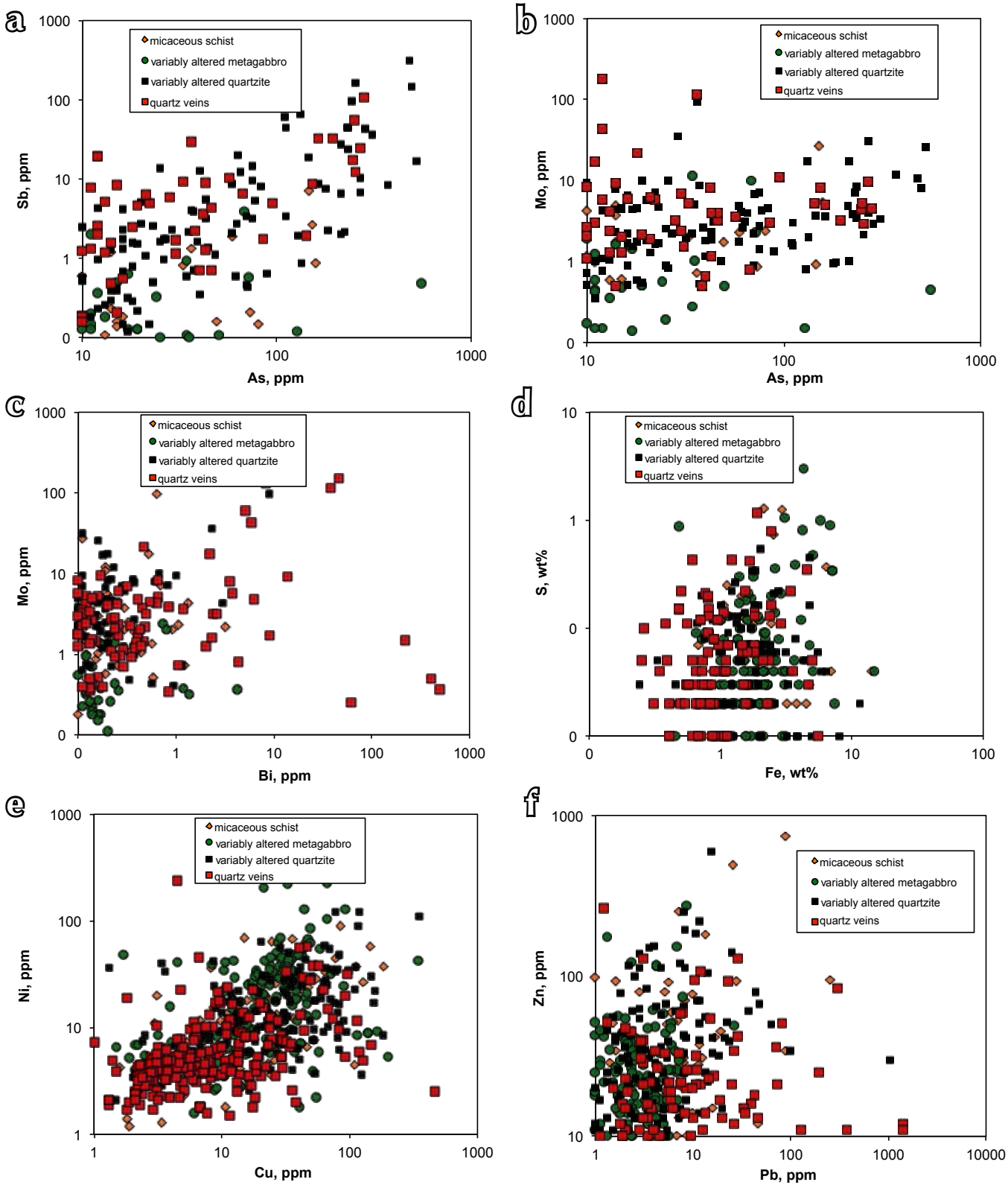

Figure 9. *Geochemical plots of metal contents of variably altered and gold mineralized rocks from near metagabbro boundaries. (a) As vs Sb; (b) As vs Mo; (c) Bi vs Mo; (d) Fe vs S; (e) Cu vs Ni; (f) Pb vs Zn.*

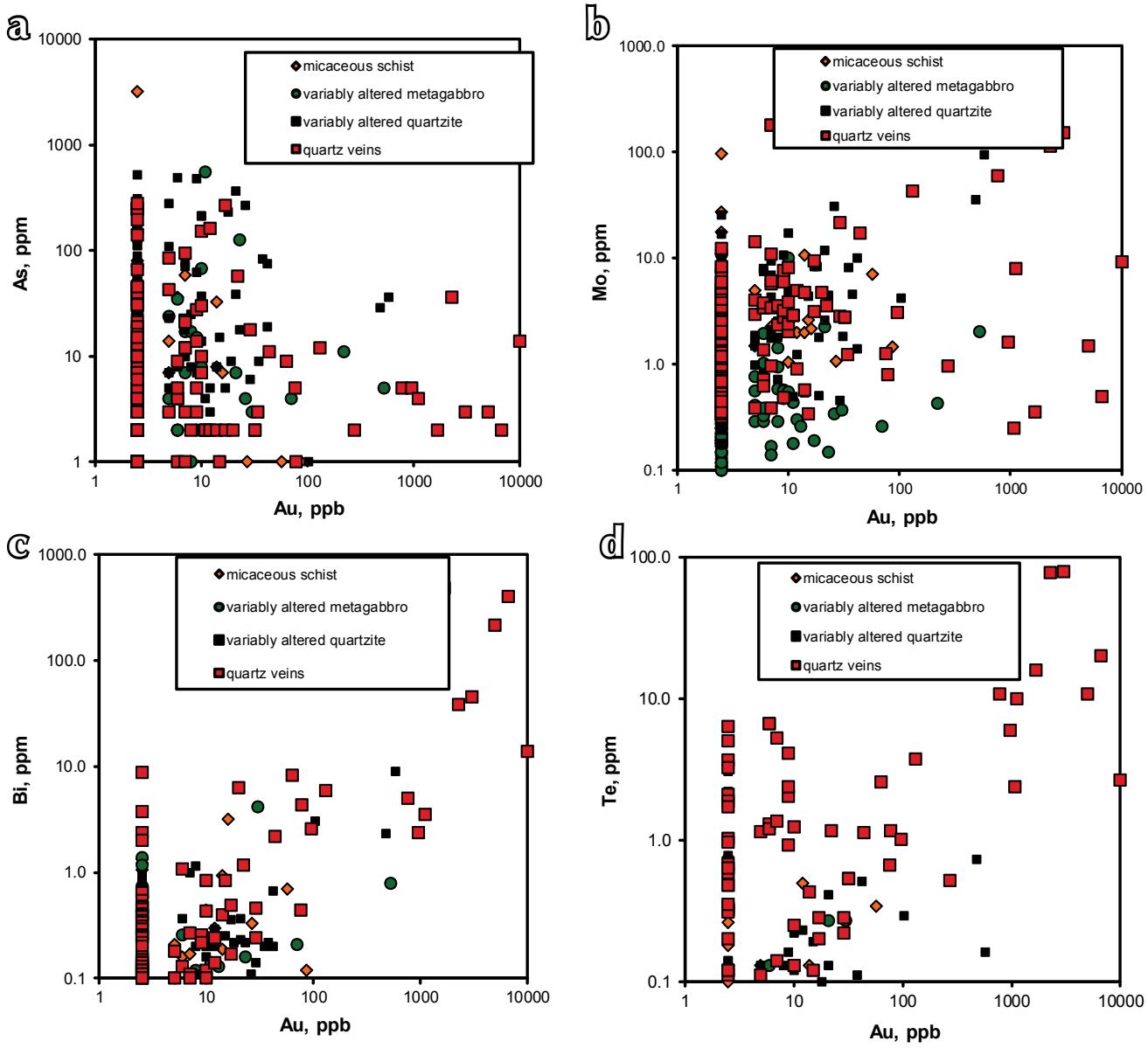

Figure 10. *Gold concentrations in variably altered rocks from near metagabbro boundaries, in relation to: a) As; b) Mo; c) Bi; and d) Te.*

DISCUSSION

CHEMICAL MOBILITY AT MAFIC BODY MARGINS

The metagabbro margins are zones with strong geochemical contrasts, between strongly mafic compositions and siliceous, micaceous, and/or calcareous compositions. Consequently, there has been some elemental exchange between these disparate rock types, on at least the metre scale and possibly greater spatial scales. The details of this migration are difficult to define because the primary rock compositions are unknown and variable. The most obvious manifestation of chemical mobility is that of syn-metamorphic K migration, resulting in development of biotite-rich foliation (Fig. 6c). This K migration must have occurred in zones up to tens of metres wide, both at mafic body margins and within the bodies where granitoid intrusions were deformed along with the mafic rocks. Likewise, metamorphic hornblende in quartzite close to (<10 m from) metagabbro margins reflects migration of mafic major elements such as Fe, Mg, and Ca from the mafic bodies.

Some altered metagabbro is moderately enriched in As compared to background levels (<20 ppm) in unaltered rocks (Fig. 9a). This As has almost certainly migrated from adjacent (<20 m) quartzite that is a relatively As-rich protolith and has As-rich quartz veins (Fig. 9a; MacKenzie *et al.,* 2010). Antimony is also enriched in the quartzite, and apparently has not migrated with the As into the metagabbro.

Graphite is most abundant in quartzite adjacent to (<50 m) metagabbro bodies, and graphite is rare or absent from quartzite more distant from metagabbro. This may be, at least partially, an artifact of poor exposure and/or weathering. However, there may also be a genetic relationship between graphite enrichment and the mafic/metasediment boundaries, facilitated by the chemical gradients at these boundaries. The latter possibility could arise because of geochemical processes that occur at these boundaries during metamorphism and subsequent alteration. Rather than being derived from a primary (sedimentary) carbon source, the graphite may have been deposited by combined oxidation-reduction reactions that occurred in these geochemically diverse boundary zones during metamorphism and/or subsequent hydrothermal alteration (Evans *et al.,* 2006; Huizenga, 2011). One speculative possibility for this process is the recrystallization of pyrrhotite to pyrite (oxidation) combined with reduction of metamorphic carbon dioxide (*e.g.*, from nearby marble), to give a reaction of the form:

1. $4FeS\ (pyrrhotite) + 4H_2S\ (dissolved) + CO_2\ (dissolved) \Rightarrow 4FeS_2\ (pyrite) + C\ (graphite) + 2H_2O + 2H_2$

Syn-metamorphic pyrrhotite is commonly seen to be replaced by late or post-metamorphic pyrite in all rock types of this study, so there is some observational support for this type of reaction. This, or some similar reaction, must have also occurred during post-metamorphic alteration, where substantial hydrothermal graphite addition has occurred in brecciated rocks (Fig. 4c; MacKenzie *et al.,* 2010).

RHEOLOGICAL CONTROL OF DEFORMATION AND FLUID FLOW

The geological history of the metagabbro boundaries is one of progressive localized deformation and rheological weakening that has

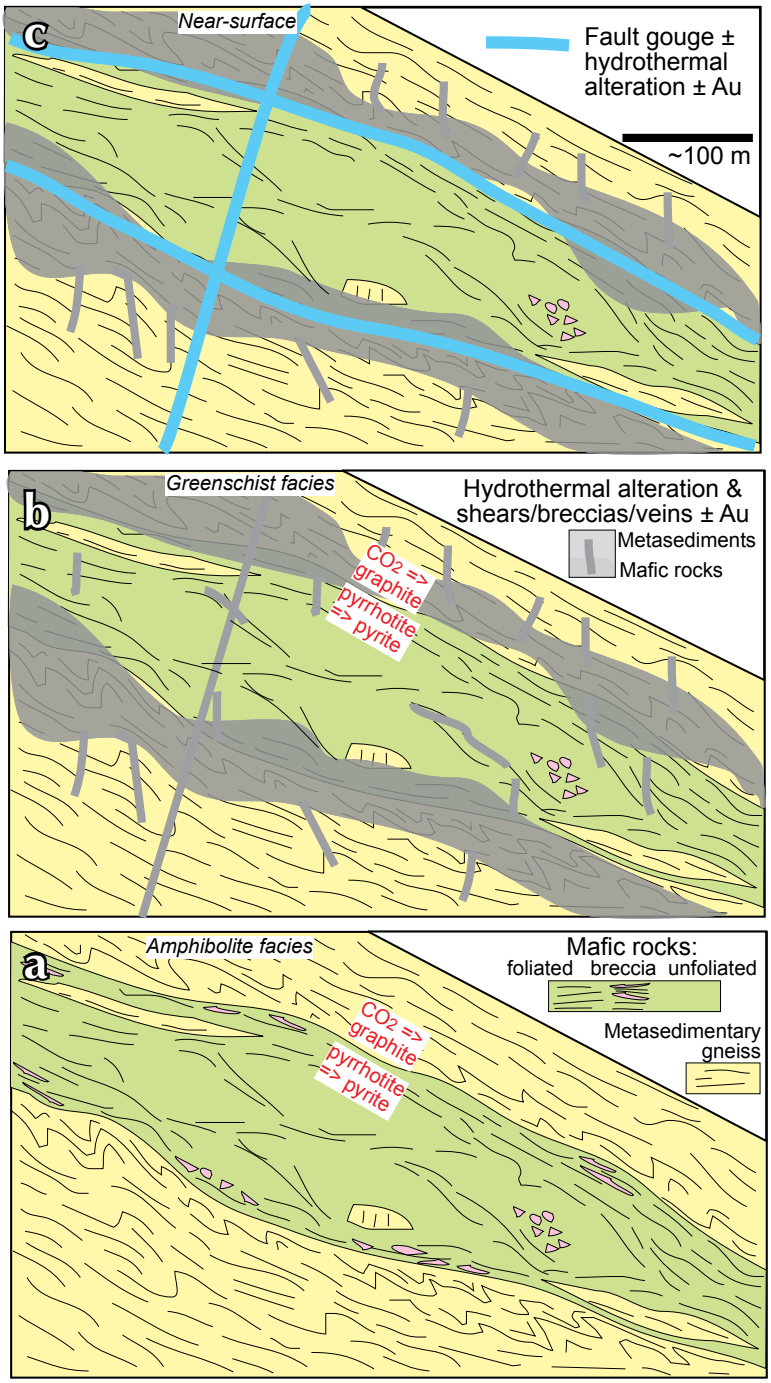

Figure 11. *Cartoon summary of the principal structural preparation events that led to permeability development in metagabbro hosted in quartzite. a) Paleozoic metamorphism and initial foliation development. Late metamorphic folding and foliation development is enhanced at the lithologic boundary and in magmatic breccia (granitoid = pink). b) Mesozoic metamorphic retrogression and hydrothermal alteration is focused in foliated rocks. c) Post-metamorphic brittle deformation and hydrothermal alteration is partly controlled by pre-existing structures.*

resulted in pronounced structural superposition zones on the 1-20 m scale. These structurally weakened zones have facilitated passage of hydrothermal fluids that have deposited veins in extensional sites and altered the immediate host rocks to varying degrees. The geometry of these metagabbro bodies and the sequence of deformation events are summarized in cartoon form in Figure 11a-c.

The earliest stages of deformation of the metagabbro bodies occur during Paleozoic metamorphism (Fig. 11a). The original mafic intrusions were dominated by pyroxene and feldspar, and this resulted in a strong competency contrast between these bodies and adjacent rocks that were rich in quartz, mica, and/or calcite. The resultant high strain gradients at the margins of the metagabbro enhanced metamorphic fluid flow and metamorphic transformations at the boundaries (Fig. 11a). These processes occurred at the centimetre to metre scale in xenolithic breccia (Fig. 7a-c), and at the metre to ten metre scale on gabbro margins (Fig. 11a). Coupled metamorphic reactions between mafic rocks and quartzite resulted in reduction of CO_2 to graphite while pyrrhotite transformed to pyrite (Fig. 11a; equation 1). Pods of some of the metagabbro remained unfoliated (Fig. 11a). Additional localized deformation, elemental mobility, and foliation development occurred around rafts of metasedimentary gneiss at and near the metagabbro margins (Fig. 11a). Late metamorphic deformation focused folding and extra late-stage foliation development in the adjacent host rocks (Fig. 11a).

Foliated metagabbro and associated folded and foliated metasedimentary gneiss were relatively permeable to incursion of hydrothermal fluids that started during greenschist facies overprinting of the metamorphic pile in the Jurassic (Table 1; Fig. 11b). This overprinting is not pervasive, even along the metagabbro margins, and variably affected metagabbro and host rocks. Later, but probably still Mesozoic, hydrothermal fluid flow was controlled by foliation and fractures within the metagabbro bodies, especially those associated with granitoid, and along metagabbro margins. These hydrothermal events (Table 2) evolved to lower temperature orogenic-hydrothermal alteration and vein formation. Veins filled extensional sites in metagabbro, associated granitoid, and immediate host rocks, with minor rock alteration (Fig. 11b). Additional hydrothermal graphite deposition occurred in adjacent quartzite (Figs. 4c and 11b).

The folded, foliated, and hydrothermally altered zones along metagabbro margins, and locally within metagabbro bodies, were subsequently the principal locus for development of late stage faults in the metamorphic rock mass, probably in the Cenozoic (Fig. 11c). These faults apparently had low net displacement, which is largely sub-parallel to the foliation (Fig. 11c). The resultant fault zones are dominated by cataclasite and gouge made up of variably altered and veined rocks from metagabbro and host rocks. This deformation has disrupted parts of the early hydrothermal alteration zones, but additional hydrothermal fluid flow has partially cemented some cataclasite. This late stage hydrothermal mineralization is not as widespread as the earlier stages, and may have been localized by specific crosscutting fault structures, in the same way as the White River gold mineralization was controlled largely by east-striking faults (MacKenzie *et al.,* 2010).

LOCALIZATION AND STYLE OF GOLD MINERALIZATION

The observed quartz veins and associated breccia have structural and textural characteristics of orogenic gold deposits (Goldfarb *et al.,* 2005), albeit only identified at a small scale in the metagabbro bodies thus far. The veins are discontinuous, and fill localized extensional sites in foliated metagabbro bodies. As such, these veins resemble the orogenic veins of the Klondike goldfield, rather than the largely vein-free disseminated gold deposits of the White River area (Fig. 1; MacKenzie *et al.,* 2010). Hydrothermal alteration of Klondike mafic schist host rocks occurred on the metre scale adjacent to veins (MacKenzie *et al.,* 2008b, MacKenzie and Craw, 2012), but hydrothermal fluids obtained only limited penetration into the mafic rocks described in this study, and alteration was extremely limited (cm scale). Some mineralized quartz veins, also with orogenic style, do occur in the margins of metabasic rocks in the White River mineralized zones, similar to those described in this study. However, most hydrothermal interaction with White River mafic rocks resulted in fuchsite alteration and no gold (MacKenzie *et al.,* 2010; Table 1).

There has been little or no As or Sb enrichment associated with hydrothermal gold mineralization at metagabbro margins in this study (Fig. 10a), similar to the As-poor orogenic gold mineralization in the Klondike area (MacKenzie *et al.,* 2008a,b). In contrast, both As and Sb are enriched to varying degrees in the White River hydrothermal gold deposits (MacKenzie *et al.,* 2010). Gold mineralization in this study involved significant Mo and Bi enrichment, both metals that are also enriched at White

River (MacKenzie *et al.,* 2010). Some of the banded pyritic quartz veins described in metagabbro bodies in this study resemble epithermal vein styles, rather than orogenic veins, although no definitive gold anomalies specifically associated with these veins have yet been determined.

CONCLUSIONS

Structurally-induced permeability to hydrothermal fluids developed in mafic intrusions in amphibolite facies basement after a protracted series of events. Paleozoic foliation development in these massive rocks initially required small-scale (centimetre-metre) elemental migration, particularly of potassium, to form biotite from primary pyroxene via metamorphic hornblende. Foliation developed around pods of rheologically more resistant mafic rocks that include coarse-grained pyroxenite differentiates. Quartzite host rocks appear to contain enhanced metamorphic graphite contents near to boundaries between quartzite and mafic bodies. Graphite deposition may have resulted from linking of redox reactions at these boundaries, involving transformation of abundant primary and metamorphic pyrrhotite to pyrite.

The amphibolite facies foliation was reworked by Jurassic deformation under greenschist facies conditions, with replacement of biotite by chlorite and muscovite. Additional graphite deposition occurred in late greenschist facies breccia in quartzite adjacent to mafic bodies, probably from the same linkage of redox reactions involving the pyrrhotite-pyrite transformation. The first stage of gold mineralization occurred during and/or after this retrogressive alteration, with emplacement of massive quartz veinlets controlled by the reworked foliation. Quartz vein emplacement was mediated by rheological contrasts at the mafic body margins, and veins nucleated preferentially in and around metagranitoid in deformed magmatic breccia. These quartz veins contain minor pyrite, and are locally enriched in Au, Bi, Mo, and Te. Gold deposition may have been facilitated by the relatively reduced chemical environment maintained by pyrrhotite-bearing mafic rocks and graphite and pyrrhotite bearing adjacent quartzite.

Later brittle deformation of the mafic rock margins facilitated several further vein formation generations, through to late stage veinlets, breccia, and alteration zones with epithermal style. The occurrence of gold in these generations is unknown, but similar generations of epithermal style alteration zones, breccia, and veins in metagranitoid host rocks near Gabbro Ridge (Fig. 3) do contain gold. It is notable that none of the hydrothermal alteration and vein formation events resulted in significant introduction of As into the mafic rocks, and gold mineralization was not accompanied by addition of anomalous As or Sb. The hosting quartzite has a relatively high As and Sb background, and these elements appear to have been largely immobile throughout the hydrothermal processes that affected the immediately adjacent mafic rocks.

ACKNOWLEDGEMENTS

This research was supported financially by Smash Minerals Corporation, the New Zealand Ministry for Science and Innovation, and the University of Otago. Discussions with Chris Siron, Chris Pennimpede, Phil Smerchanski, Rob Mackie, Dennis Arne, Mike Cooley, Lamont Leatherman, Kristy Long, and Mike Young helped us to develop geological ideas expressed herein. Olivia Brown provided excellent technical assistance.

REFERENCES

Chapman, R.J., Mortensen, J.K., and LeBarge, W.P., 2011. Styles of lode gold mineralization contributing to the placers of the Indian River and Black Hills Creek, Yukon Territory, Canada as deduced from microchemical characterization of placer gold grains. Mineralium Deposita, vol. 46, p. 881-903.

Evans, K.A., Phillips, G.N., and Powell, R., 2006. Rock-buffering of auriferous fluids in altered rocks associated with the Golden Mile-style mineralization, Kalgoorlie gold field, Western Australia. Economic Geology, vol. 101, p. 805-817.

Fuller, E.A. and Andersen, F.J., 1992. Placer geology of Black Hills Creek (parts of 1150/7 &10). Yukon Exploration and Geology 1993, Exploration and Geological Services Division, Indian and Northern Affairs Canada, p. 33–38.

Gabrielse, H., Murphy, D.C., and Mortensen, J.K., 2006. Cretaceous and Cenozoic dextral orogen-parallel displacements, magmatism, and paleogeography, north-central Canadian Cordillera. *In:* Paleogeography of the North American Cordillera: Evidence For and Against Large-Scale Displacments, J.W. Haggart, R. J. Enkin, and J.W.H. Monger (eds.), Geological Association of Canada, Special Paper 46, p. 255-276

Gabrielse, H. and Yorath, C.J., 1991. Tectonic synthesis, Chapter 18. *In:* Geology of the Cordilleran Orogen in Canada, H. Gabrielse and C.J. Yorath (eds.), Geology of Canada, vol. 4, p. 677–705.

Goldfarb, R.J., Baker, T., Dube, B., Groves, D.I., Hart, C.J.R., and Gosselin, P., 2005. Distribution, character and genesis of gold deposits in metamorphic terranes. *In*: Economic Geology 100th Anniversary Volume, J.W. Hedenquist, J.F.H. Thompson, R.J. Goldfarb, and J.P. Richards (eds.), Economic Geology, p. 407-450.

Huizenga, J.-M., 2011. Thermodynamic modelling of a cooling C–O–H fluid–graphite system: implications for hydrothermal graphite precipitation. Mineralium Deposita, vol. 46, p. 23-33.

Lowey, G.W. 2005. The origin and evolution of the Klondike goldfields, Yukon, Canada. Ore Geology Reviews, vol. 28, p. 431-450.

MacKenzie, D., Craw, D., and Mortensen, J.K., 2008a. Structural controls on orogenic gold mineralisation in the Klondike goldfield, Canada. Mineralium Deposita, vol. 43, p. 435-448.

MacKenzie, D., Craw, D., Mortensen, J.K., and Liverton, T., 2008b. Disseminated gold mineralisation associated with orogenic veins in the Klondike Schist, Yukon. *In:* Yukon Exploration and Geology 2007, D.S. Emond, L.R. Blackburn, R.P. Hill, and L.H. Weston (eds.), Yukon Geological Survey, p. 215-224.

MacKenzie, D., Craw, D., Cooley, M., and Fleming, A., 2010. Lithogeochemical localisation of disseminated gold in the White River area, Yukon, Canada. Mineralium Deposita, vol. 45, p. 683-705.

MacKenzie, D. and Craw, D., 2012. Contrasting structural settings of mafic and ultramafic rocks in the Yukon-Tanana terrane. *In:* Yukon Exploration and Geology 2011, K.E. MacFarlane and P.J. Sack (eds.), Yukon Geological Survey, p. 115-127.

Mortensen, J.K., 1990. Geology and U-Pb chronology of the Klondike District, west-central Yukon. Canadian Journal of Earth Sciences, vol. 27, p. 903-914.

Mortensen, J.K., 1992. Pre-mid-Mesozoic tectonic evolution of the Yukon-Tanana Terrane, Yukon and Alaska. Tectonics, vol. 11, p. 836-853.

Mortensen, J.K., 1996. Geological compilation maps of the northern Stewart River map area, Klondike and Sixtymile Districts (115N/15, 16; 1150/13,14; and parts of 1150/15, 16). Exploration and Geological Services Division, Yukon Region, Indian and Northern Affairs Canada, Open File 1996-1(G), 43 p.

Ruks, T.W., Piercey, S.J., Ryan, J.J., Villeneuve, M.E., and Creaser, R.A., 2006. Mid to late Paleozoic K-feldspar augen granitoids of the Yukon-Tanana Terrane, Yukon, Canada: Implications for crustal growth and tectonic evolution of the northern Cordillera. GSA Bulletin 118, p. 1212-1231.

Ryan, J.J. and Gordey, S.P., 2004. Geology, Stewart River Area (Parts of 115 N/1,2,7,8 and 115-O/2–12), Yukon Territory. Geological Survey of Canada, Open File 4641, scale 1:100 000.

Wainwright, A.J., Simmons, A.T., Finnigan, C.S., Smith, T.R., and Carpenter, R.L., 2011. Geology of new gold discoveries in the Coffee Creek area, White Gold district, west-central Yukon. *In:* Yukon Exploration and Geology 2010, K.E. MacFarlane, L.H. Weston and C. Relf (eds.), Yukon Geological Survey, p. 233-247.